ISCI, Volume *21*

Supplemental Information

Secretagogin Regulates Insulin Signaling by Direct Insulin Binding

Anand Kumar Sharma, Radhika Khandelwal, M. Jerald Mahesh Kumar, N. Sai Ram, Amrutha H. Chidananda, T. Avinash Raj, and Yogendra Sharma

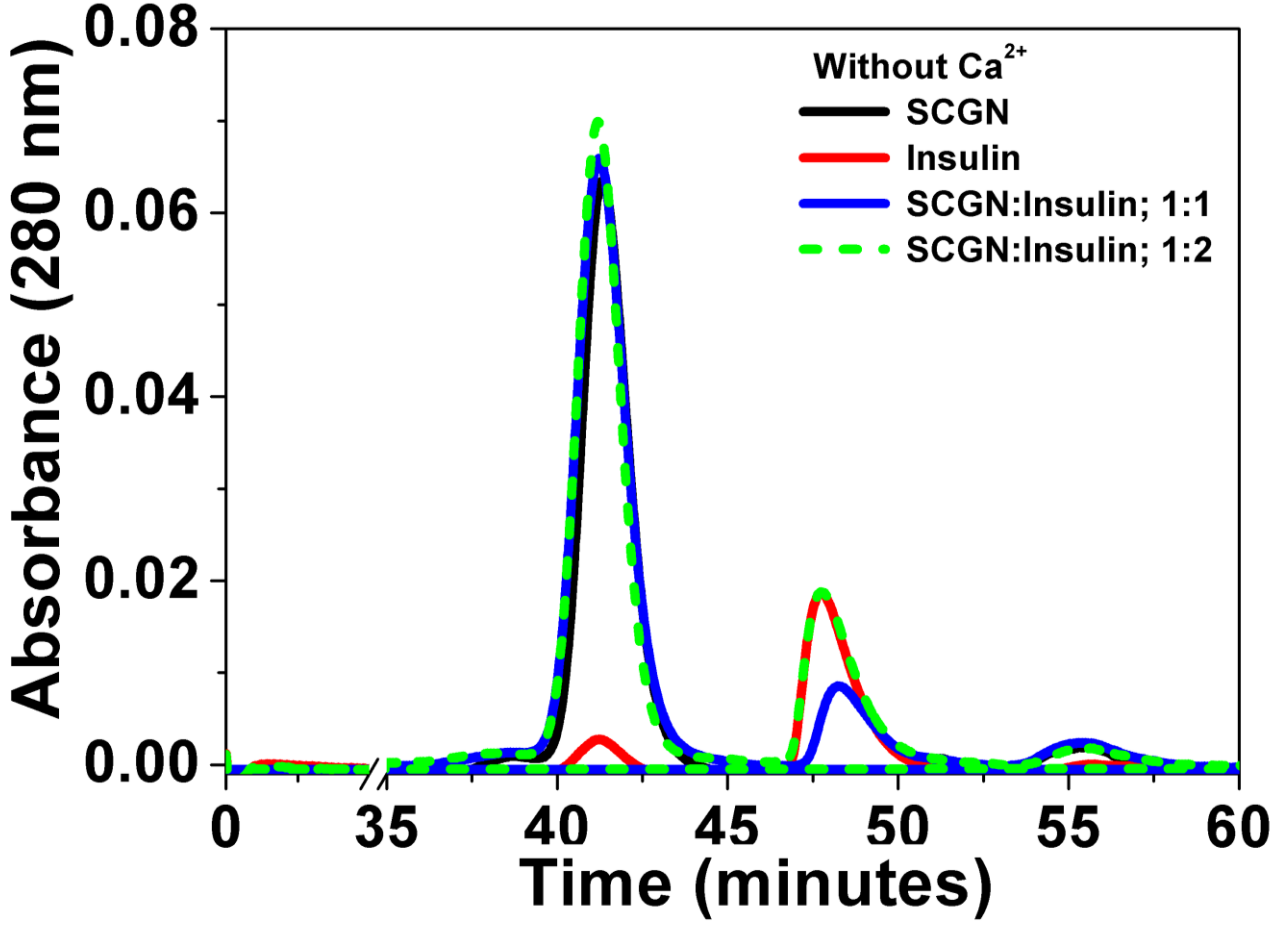
Without Ca2+
SCGN
Insulin
SCGN:Insulin; 1:1
SCGN:Insulin; 1:2
Absorbance (280 nm)
0.08
0.06
0.04
0.02
0.00
0
35
40
45
50
55
60
Time (minutes)

Fig. S1

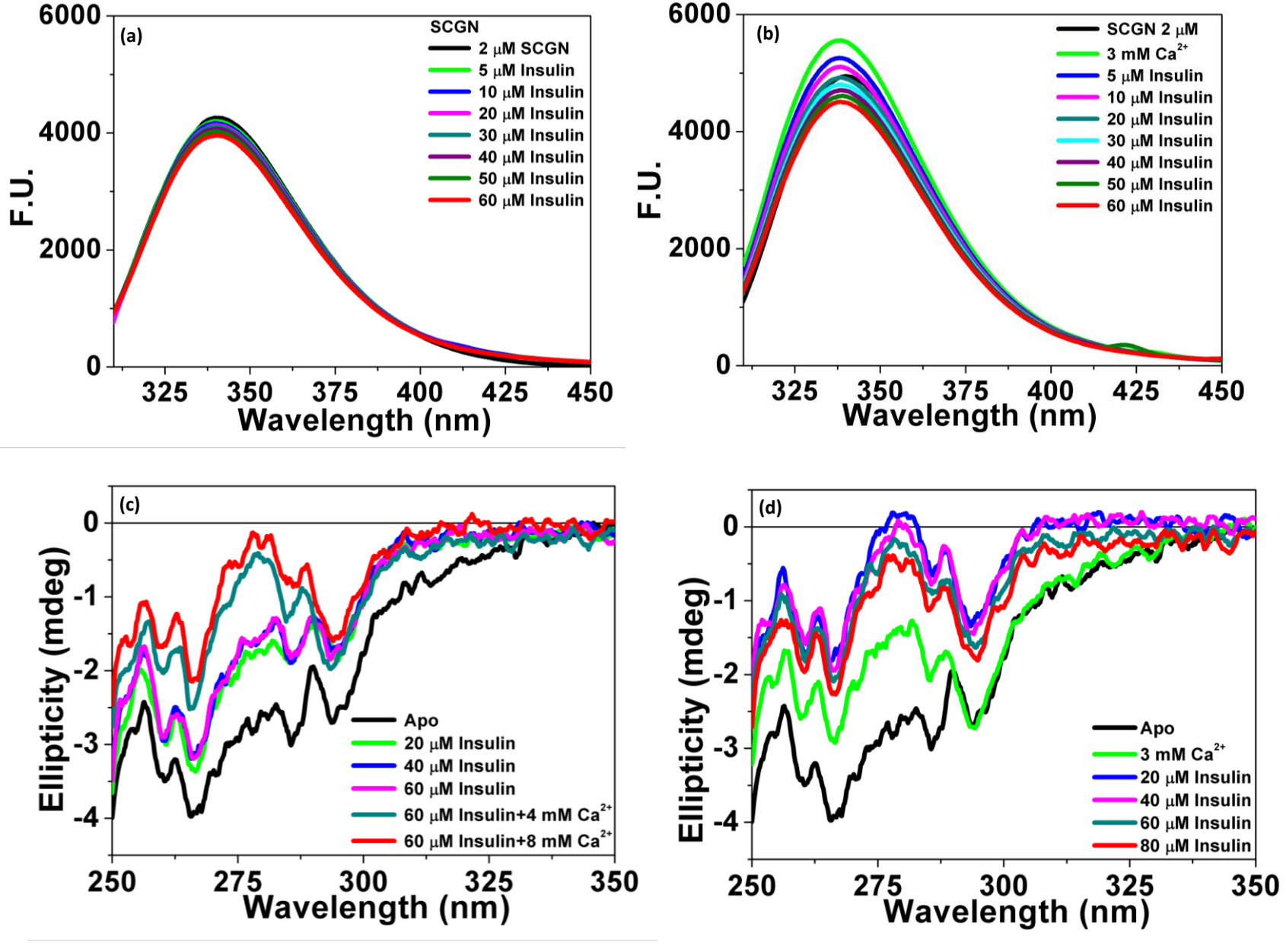
(a)
SCGN
2 μM SCGN
5 μM Insulin
10 μM Insulin
20 μM Insulin
30 μM Insulin
40 μM Insulin
50 μM Insulin
60 μM Insulin
F.U.
Wavelength (nm)
(b)
SCGN 2 μM
3 mM Ca2+
5 μM Insulin
10 μM Insulin
20 μM Insulin
30 μM Insulin
40 μM Insulin
50 μM Insulin
60 μM Insulin
F.U.
Wavelength (nm)
(c)
Apo
20 μM Insulin
40 μM Insulin
60 μM Insulin
60 μM Insulin+4 mM Ca2+
60 μM Insulin+8 mM Ca2+
Ellipticity (mdeg)
Wavelength (nm)
(d)
Apo
3 mM Ca2+
20 μM Insulin
40 μM Insulin
60 μM Insulin
80 μM Insulin
Ellipticity (mdeg)
Wavelength (nm)

Fig. S2

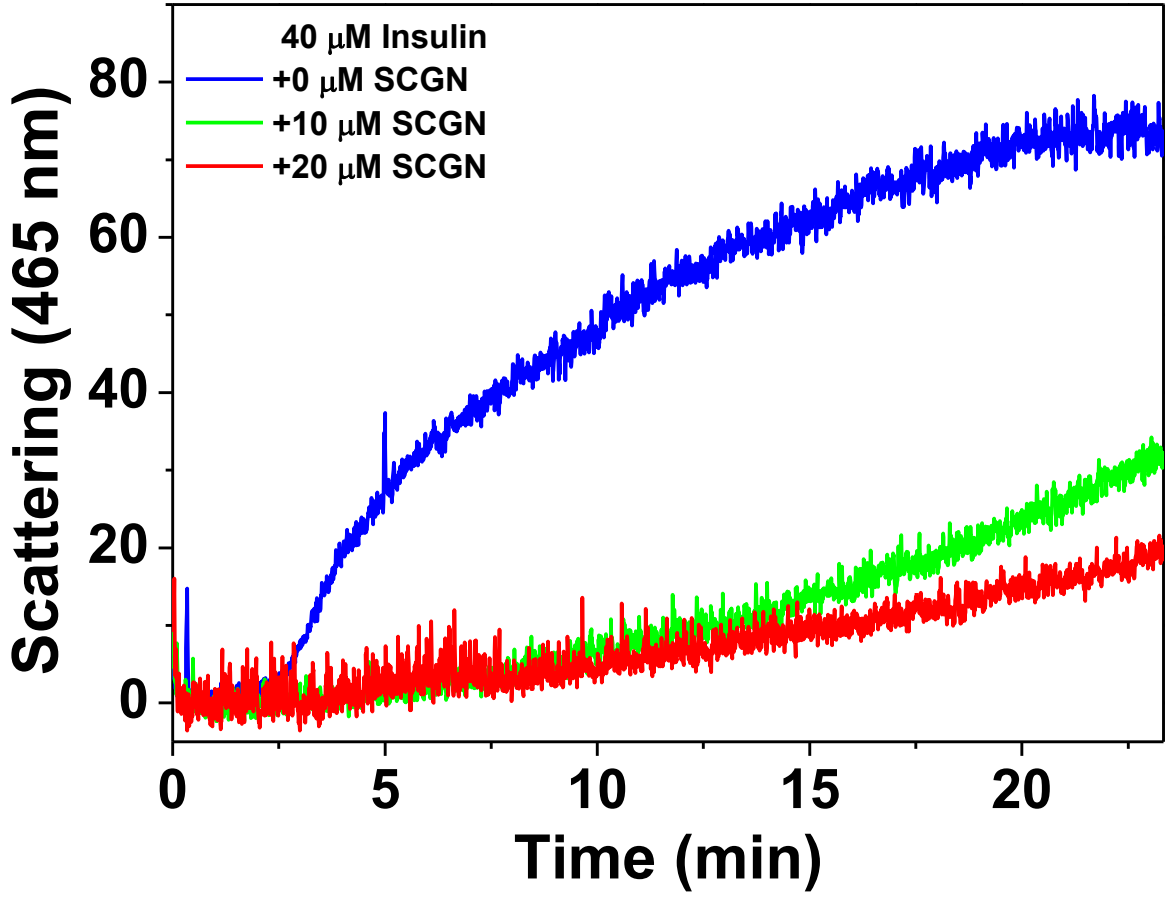
40 μM Insulin
+0 μM SCGN
+10 μM SCGN
+20 μM SCGN
Scattering (465 nm)
0
20
40
60
80
0
5
10
15
20
Time (min)

Fig. S3

Differentiated C2C12 myotubes

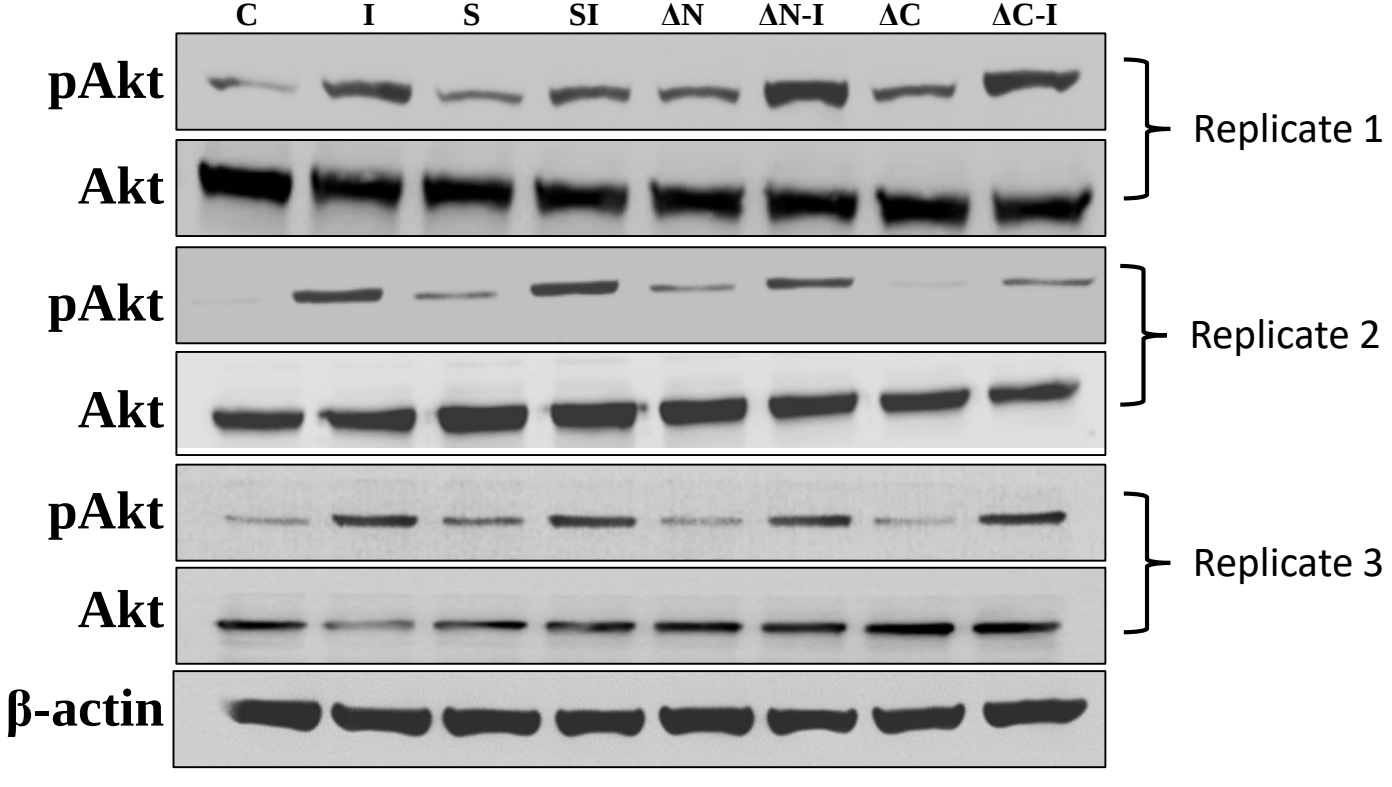

Fig. S4

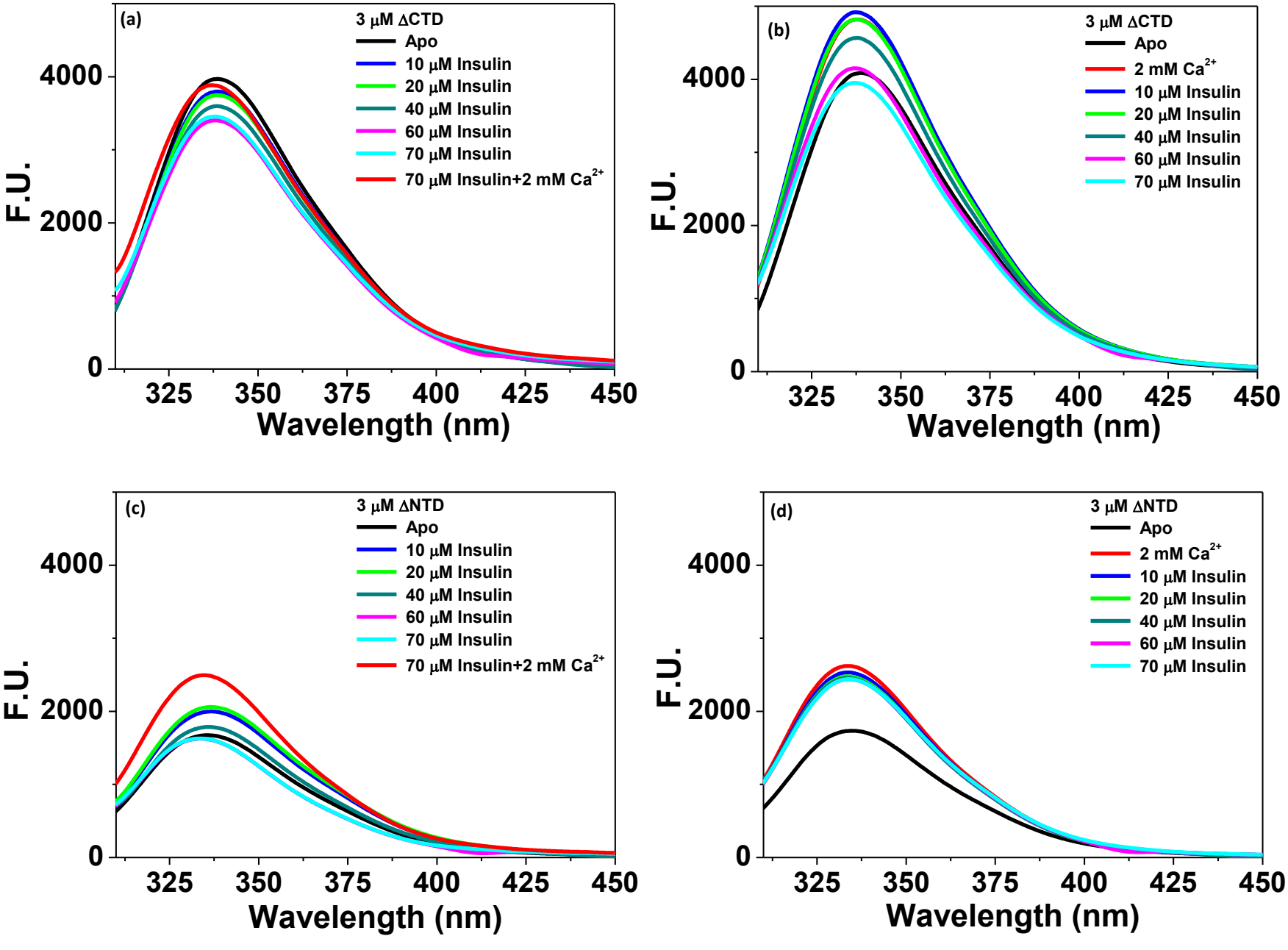
(a)
3 μM ΔCTD
Apo
10 μM Insulin
20 μM Insulin
40 μM Insulin
60 μM Insulin
70 μM Insulin
70 μM Insulin+2 mM Ca2+
F.U.
Wavelength (nm)
(b)
3 μM ΔCTD
Apo
2 mM Ca2+
10 μM Insulin
20 μM Insulin
40 μM Insulin
60 μM Insulin
70 μM Insulin
F.U.
Wavelength (nm)
(c)
3 μM ΔNTD
Apo
10 μM Insulin
20 μM Insulin
40 μM Insulin
60 μM Insulin
70 μM Insulin
70 μM Insulin+2 mM Ca2+
F.U.
Wavelength (nm)
(d)
3 μM ΔNTD
Apo
2 mM Ca2+
10 μM Insulin
20 μM Insulin
40 μM Insulin
60 μM Insulin
70 μM Insulin
F.U.
Wavelength (nm)

Fig. S5

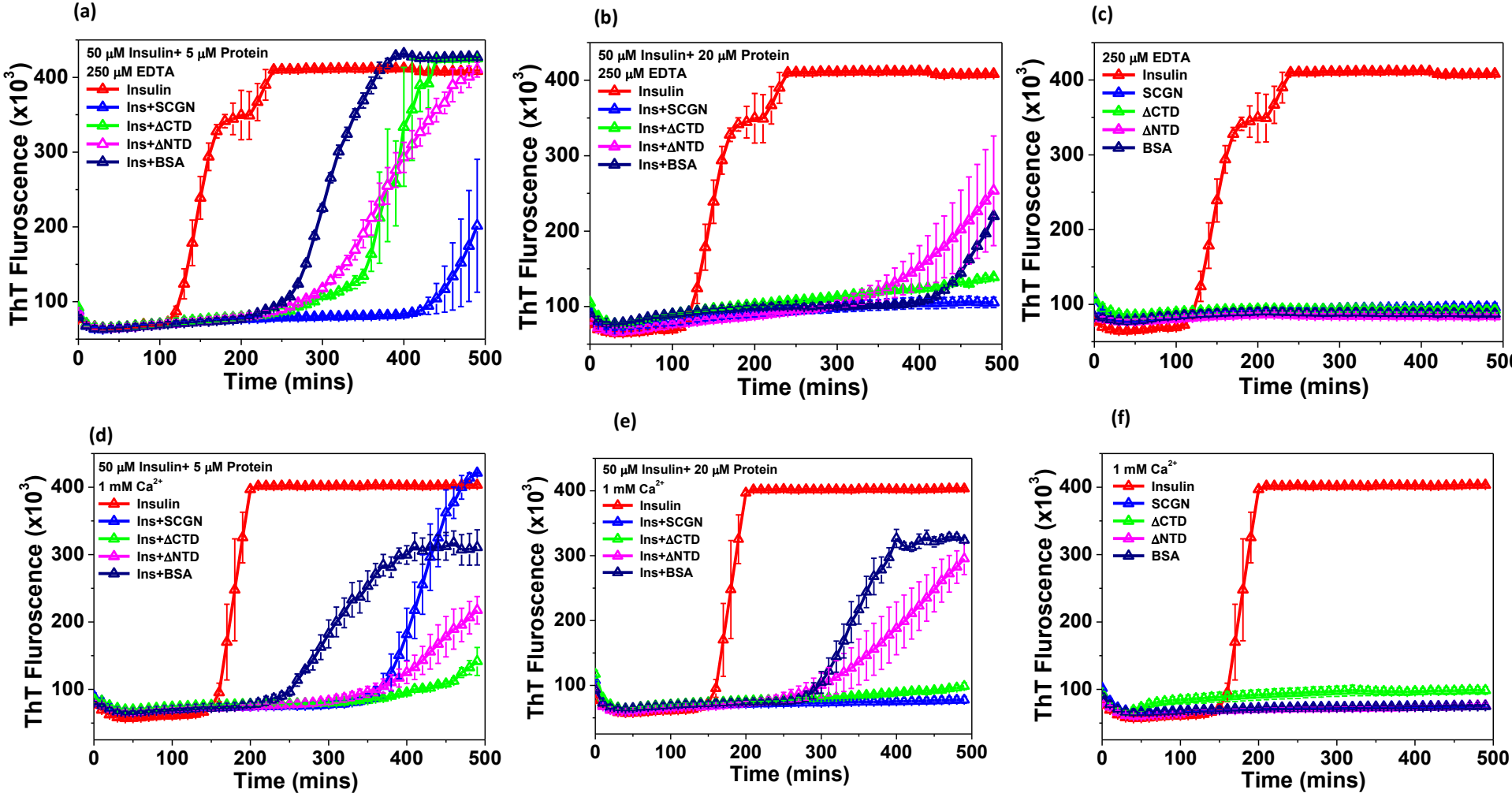
(a)
50 μM Insulin+ 5 μM Protein
250 μM EDTA
Insulin
Ins+SCGN
Ins+ΔCTD
Ins+ΔNTD
Ins+BSA
ThT Fluroscence (x10^3)
Time (mins)
(b)
50 μM Insulin+ 20 μM Protein
250 μM EDTA
Insulin
Ins+SCGN
Ins+ΔCTD
Ins+ΔNTD
Ins+BSA
ThT Fluroscence (x10^3)
Time (mins)
(c)
250 μM EDTA
Insulin
SCGN
ΔCTD
ΔNTD
BSA
ThT Fluroscence (x10^3)
Time (mins)
(d)
50 μM Insulin+ 5 μM Protein
1 mM Ca2+
Insulin
Ins+SCGN
Ins+ΔCTD
Ins+ΔNTD
Ins+BSA
ThT Fluroscence (x10^3)
Time (mins)
(e)
50 μM Insulin+ 20 μM Protein
1 mM Ca2+
Insulin
Ins+SCGN
Ins+ΔCTD
Ins+ΔNTD
Ins+BSA
ThT Fluroscence (x10^3)
Time (mins)
(f)
1 mM Ca2+
Insulin
SCGN
ΔCTD
ΔNTD
BSA
ThT Fluroscence (x10^3)
Time (mins)

Fig. S6

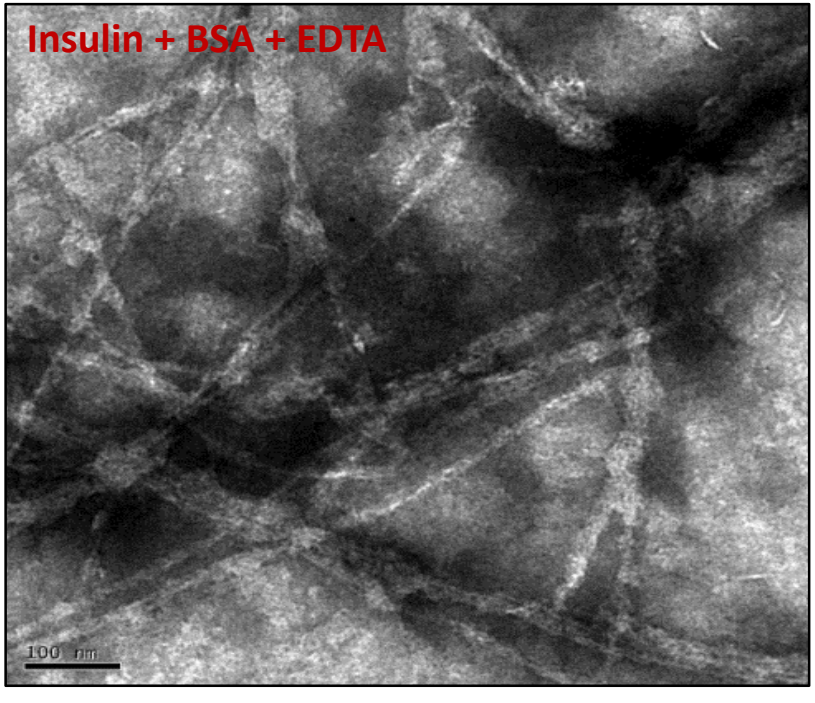

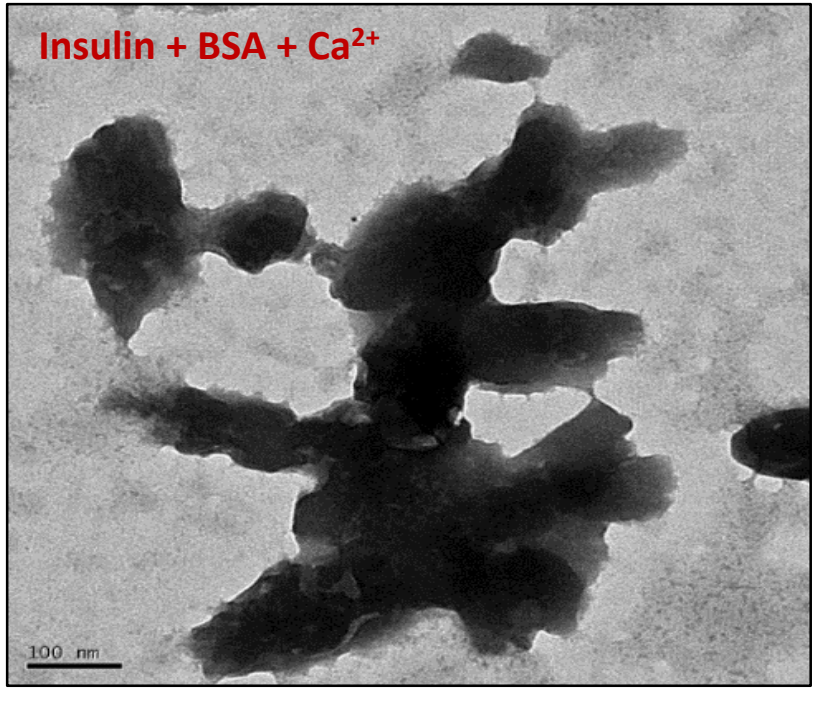

Fig. S7

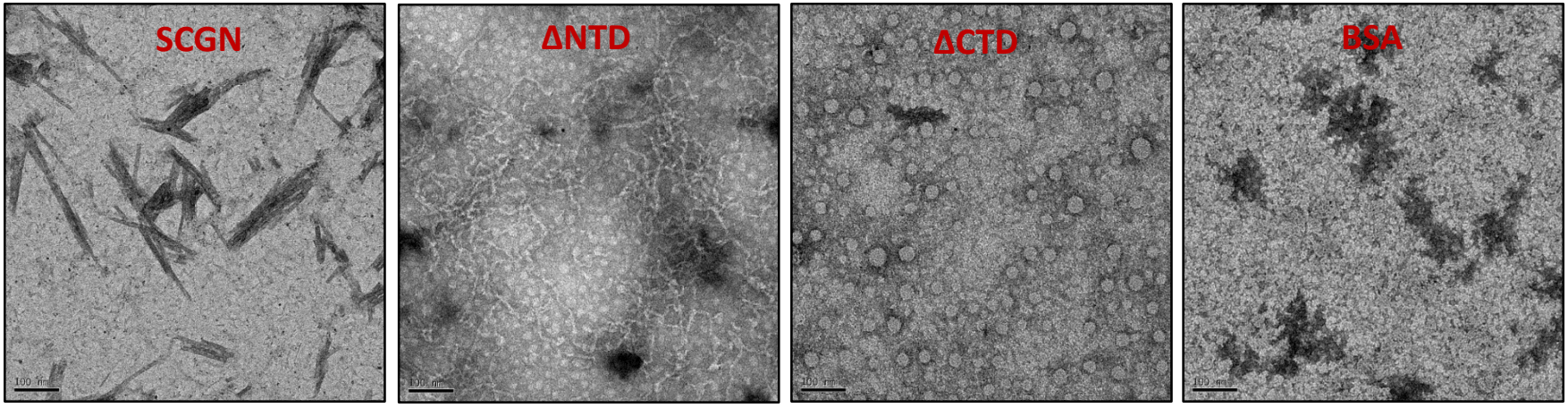

Fig. S8

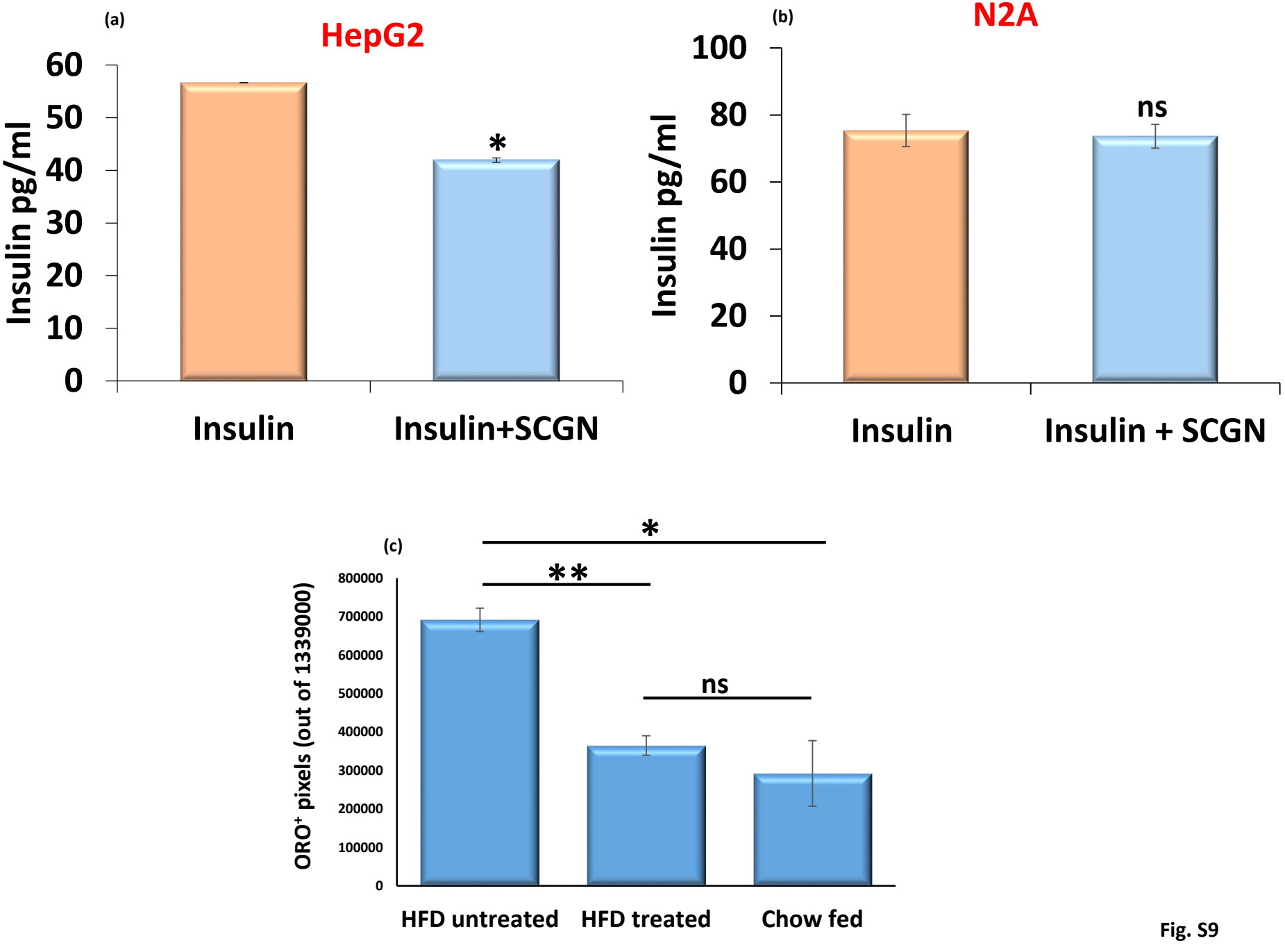
(a)
HepG2
Insulin pg/ml
60
50
40
30
20
10
0
*
Insulin
Insulin+SCGN
(b)
N2A
Insulin pg/ml
100
80
60
40
20
0
ns
Insulin
Insulin + SCGN
(c)
*
**
ns
ORO+ pixels (out of 1339000)
800000
700000
600000
500000
400000
300000
200000
100000
0
HFD untreated
HFD treated
Chow fed

Fig. S9

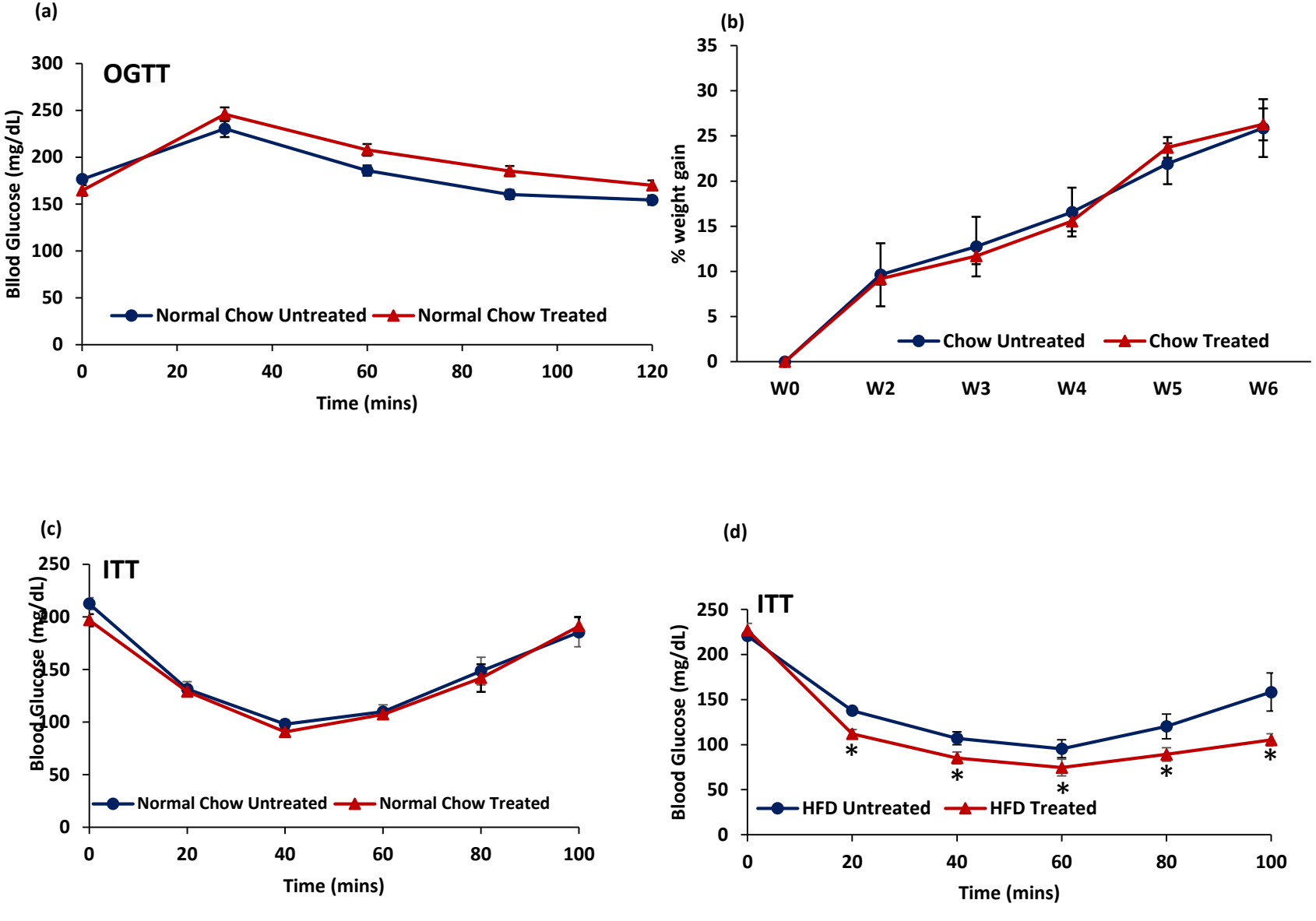
(a)
OGTT
Bllod Glucose (mg/dL)
300
250
200
150
100
50
0
0
20
40
60
80
100
120
Time (mins)
Normal Chow Untreated
Normal Chow Treated
(b)
% weight gain
35
30
25
20
15
10
5
0
W0
W2
W3
W4
W5
W6
Chow Untreated
Chow Treated
(c)
ITT
Blood Glucose (mg/dL)
250
200
150
100
50
0
0
20
40
60
80
100
Time (mins)
Normal Chow Untreated
Normal Chow Treated
(d)
ITT
Blood Glucose (mg/dL)
250
200
150
100
50
0
0
20
40
60
80
100
Time (mins)
HFD Untreated
HFD Treated
*
*
*
*
*

Fig. S10

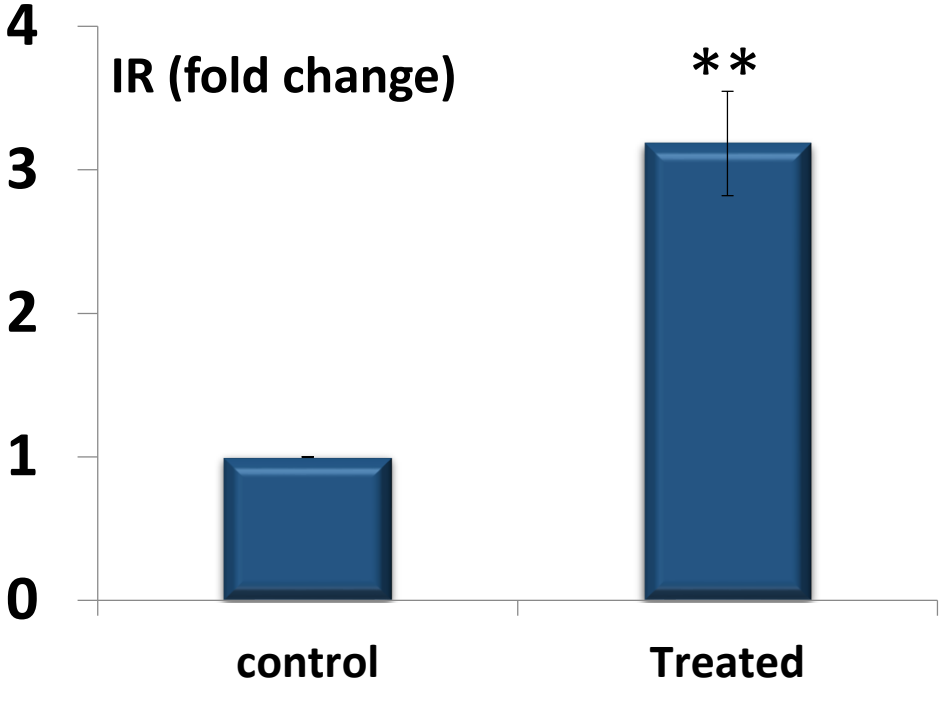

Hepatic Genes Showing unperturbed expression

- ✓ FASN
- ✓ GlucoK
- ✓ G6Pase
- ✓ Glut4
- ✓ PEPCK
- ✓ SREB1
- ✓ p85a

Fig. S11

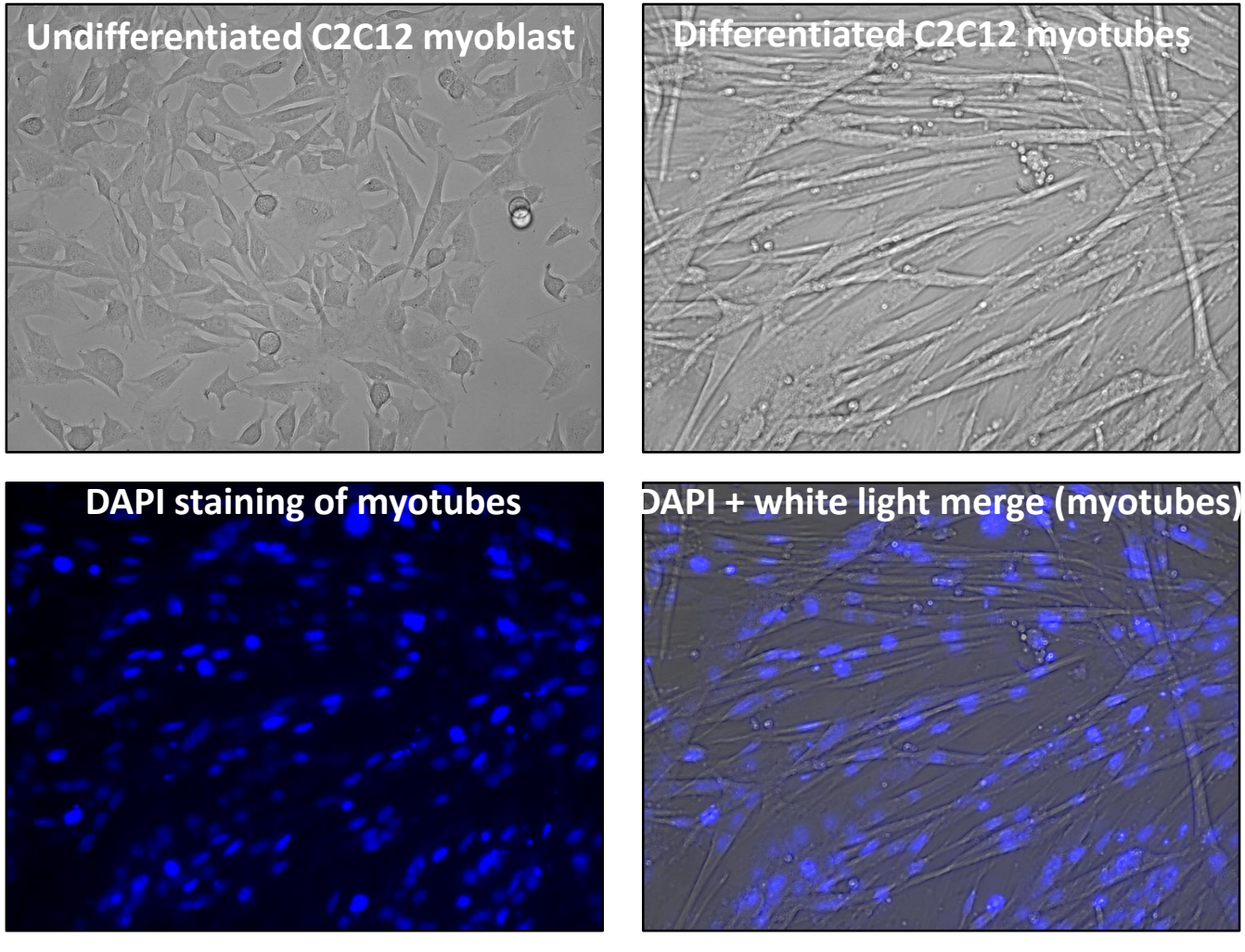
Undifferentiated C2C12 myoblast
Differentiated C2C12 myotubes
DAPI staining of myotubes
DAPI + white light merge (myotubes)

Fig. S12

Supplementary figure legends

Figure S1. Lack of stability of SCGN-insulin complex in the absence of Ca^{2+}, related to Figure 1. Analytical gel filtration elution profile of individual proteins and SCGN-insulin mixture.

Figure S2. Ca^{2+} is a positive allosteric modulator of insulin binding to SCGN, related to Figure 1. (a, b) fluorescence spectra demonstrating changes in Trp microenvironment of SCGN upon insulin titration into the apo- and holo-proteins; (c, d) Near UV-CD spectra of apo- and holo-SCGN upon insulin binding illustrating global conformational changes in the protein.

Figure S3. SCGN protects insulin from DTT induced aggregation, related to Figure 2. Change in Rayleigh scattering demonstrating the extent of insulin aggregation upon addition of DTT in the presence or absence of SCGN.

Figure S4. Central domain of SCGN modulates *in vitro* insulin response, related to Figure 4. C2C12 cells were treated with given protein/insulin combinations and Akt phosphorylation was assessed with pAkt specific antibody. Note a minimal effect of terminal-domains truncation on insulin potentiation suggesting that the central domain may have a role in modulating insulin activity *in vitro*.

Figure S5. N-terminal domain deletion impedes insulin binding, related to Figure 4. (a-d) Fluorescence spectra demonstrating changes in Trp microenvironment of truncated SCGN upon insulin titration into the apo- and holo-ΔCTD (a, b) or apo- and holo-ΔNTD (c, d). There was an appreciable reduction in insulin-induced fluorescence changes in ΔNTD.

Figure S6. N-terminal domain deletion leads to compromised insulin protection, related to Figure 4. (a-c: Ca^{2+} free conditions/d-f: Ca^{2+} rich condition). (a, b, d, e) In Insulin fibrillation as monitored by ThT dye at given protein/insulin concentrations; (c, f) ThT fluorescence of given protein in the absence of insulin. *Please note that same insulin*

aggregation profile is used in all panels of the given condition as the data is derived from the same experiment.

Figure S7. BSA does not prevent insulin fibrillation completely, related to Figure 4. (a) Insulin fibrillation TEM images in the presence of BSA (+/- Ca^{2+}).

Figure S8. SCGN or truncated proteins do not form fibrils, related to Figure 4. Individual proteins incubated under the amyloidogenic conditions do not form visible fibrils suggesting that the fibrils (seen in TEM images or ThT fluorescence) are the consequence of insulin misfolding and SCGN does not contribute to fibrillation.

Figure S9. SCGN accelerates insulin internalization, related to Figure 6. (a) HepG2 (b) N2A cells were incubated with insulin in the presence/absence of SCGN for 1 hour and then free insulin concentration was measured by ELISA; (c) Quantitation of Oil Red O staining of liver sections from HFD treated/untreated animals and control chow group.

Figure S10. SCGN administration to normal chow-fed animals is largely inconsequential, related to Figure 6. (a) OGTT; (b) weight gain (c) ITT in SCGN treated/untreated normal chow-fed animals. A trivial change in these parameters upon SCGN administration is noted. In contrast, (d) HFD-fed animals treated with SCGN for the same duration exhibit considerably better insulin tolerance as compared to HFD untreated group.

Figure S11. SCGN administration to STZ animals does not induce transcriptional changes in the liver, related to Figure 8. Insulin receptor was significantly upregulated in the liver samples of treated animals. However, the expression of other tested hepatic genes was unperturbed.

Figure S12. Generation of differentiated, multinuclear C2C12 myotubes, related to transparent methods and Figure 3. Insulin treatment followed by serum starvation for 48 hours leads to visually appreciable myotube morphology, which is validated by DAPI assisted staining of the nucleus to confirm multinuclear state of myotubes.

Table S1

Gene Name	Forward Primer (5’-3’)	Reverse Primer (5’-3’)
IR	CTCTCTGGCAGGAAATGGCT	TTGGCAATATTTGATGGGACATCT
FASN	GAGACGCTTCTGGGCTACAG	GGGCAATGCTTGGTCCTTTG
GLUCOK	TTGCAACACTCAGCCAGACA	TGAGGATAAGCAGGGGTCGT
G6Pase	GGATTCCGGTGTTTGAACGTC	GCAAGGTAGATCCGGGACAG
GLUT4	GCTCTGACGATGGGGAACC	AAACTGAAGGGAGCCAAGCA
PEPCK	CCCCCTTGTCTATGAAGCCC	GATCTTGCCCTTGTGTTCTGC
SREBP1	CGGCTCTGGAACAGACACTG	TGAGCTGGAGCATGTCTTCG
p85aPI3K	CCTGGACTTAGAGTGTGCCA	GGGCAGTGCTGGTGGAT
INS1	CTGGTGGGCATCCAGTAACC	GTTGAAACAATGACCTGCTTGC
INS2	CCATCAGCAAGCAGGAAGGTTA	GGACTCCCAGAGGAAGAGCA
PC1	CAAGGCCTGTCACCTTGGTA	GCGCTTGTTATTCGCTGGTC
SCGN	CGATGTTAGTAAAACTGGAGCCC	CAGATCCACACCACTGATGCT
PC2	TTTGGAGTCCGAAAGCTCCC	GGTGTAGGCTGCGTCTTCTT
GLUT2	GAGATCGCTCCAACCACACT	TGAGGCCAGCAATCTGACTA
HPRT1	CTTCCTCCTCAGACCGCTTT	TCATCGCTAATCACGACGCT
ACTB	GCAAGCAGGAGTACGATGAGT	AGGGTGTAAAACGCAGCTCAG

Table S1. List of qRT-PCR primers used in this study, related to Figure 8. Whenever possible, the primers were designed to span exon-exon junction.

Transparent Methods

Antibodies: Anti-SCGN (bs11754R; Bioss), anti-insulin (bs0855R; Bioss), anti-phospho-Akt (Ser473) rabbit mAb (#9018S; Cell Signalling Technology), anti-Akt (pan) rabbit mAb (#4691S; Cell Signalling Technology), anti-β-actin (bs0061R; Bioss), secondary HRP (bs0295G; Bioss), Alexa Fluor 594 Goat anti rabbit IgG (A11037; Life technologies Molecular probes).

Pull down assay: His-tagged SCGN (100 μg) was allowed to bind to a Ni-NTA resin column in the presence of Ca^{2+}. MIN6 cells were scrapped in RIPA buffer and sonicated for 10 cycles of 10 sec on/off cycle on a Sonics VibraCell sonicator at 20% efficiency. The whole MIN6 cell lysate was loaded on a SCGN-bound Ni-NTA resin column, washed with PBST buffer and eluted with 250 mM imidazole. The supernatant, wash, and eluents were resolved on 12% SDS-PAGE and gel pieces containing protein bands were excised. The samples were processed for mass spectrometry identification by desalting with zip-tip and analyzed on a Q-Exactive Thermo Scientific mass spectrometer. A protein-free resin control was run similarly. Proteins identified in resin control were considered as background and were excluded from pull down data analysis. Protein identification was performed using Xcalibur software with mouse reference protein databank (UniProt) using a high stringency. Peptide confidence was kept high with precursor mass tolerance of 5 ppm, while fragment mass tolerance was 0.05 Da. Met oxidation was selected as dynamic modification site while Cys carbamidomethylation was set as static modification.

Cell Culture: MIN6 cells were cultured in DMEM supplemented with 10% FBS, penicillin (60 mg/lit), and streptomycin (100 mg/lit). HepG2 cells were cultured in similar conditions. C2C12 myocytes were maintained in 20% serum and antibiotics. To differentiate, C2C12 cells were grown in a serum-free DMEM media containing 100 nM insulin. After 24 hours, cells were grown in serum/insulin-free DMEM for 48 hours. The differentiation was assessed by tubular morphology and multinuclear structure by DAPI staining (Fig. S13).

Colocalization: MIN6 cells ($0.2x10^6$) were seeded on coverslips in a 6-well plate. After 24 hours, cells were fixed in 4% formaldehyde and immunostained for SCGN and insulin.

Briefly, cells were washed with PBS and permeabilized with 0.1% triton X-100 followed by blocking with 2% BSA at room temperature for 1 hour. Next, the cells were incubated with the anti-insulin antibody (raised in mouse) and anti-SCGN antibody (raised in rabbit) for one hour. After washing thrice with PBST (0.1% Tween 20), cells were incubated with secondary antibodies (goat anti-rabbit Alexa Fluor 594 and goat anti-mouse Alexa Fluor 488) for 1 hour followed by five washes with PBST. DAPI (component of mounting media) was used as a nuclear staining dye. Images were captured on Leica SP8 confocal microscope. Middle three z-sections were stacked with minimum background and contrast correction using Image J software without manipulating any specific feature or part of the image.

Co-immunoprecipitation (CoIP): MIN6 cells were grown in a T75 tissue culture flask and trypsinized upon confluency. The cells collected after slow centrifugation were resuspended in lysis buffer (PBS, 0.1% Tween 20, protCEASE 50; G-Biosciences), and ruptured by three freeze-thaw cycles. and the supernatant was used for immunoprecipitation. For IP from media, 10 ml of conditioned media (from a T75 flask in which 80-90% confluent MIN6 cells were cultured for 24 hours) was concentrated using Amicon Ultrafiltration device (cut-off of 3 kDa). Subsequently, five micrograms of anti-insulin antibody (or 5 µg of irrelevant IgG) was mixed to 1 ml cell lysate (or to media) and incubated overnight at 4 ºC with continuous rotation. Antibody complex was precipitated using Protein A-Sepharose beads (Amersham Biosciences) followed by five washes with PBST. For immunoprecipitation of SCGN-insulin complex from animal plasma, we first incubated anti-insulin antibody with a pre-equilibrated (in PBST) Dynabeads for 2 hours at 4 ºC. After three washes, Dynabead was incubated overnight with mice plasma followed by five washes with PBST. The resin was boiled for 2 minutes in SDS-PAGE loading buffer centrifuged and the supernatant was resolved on 12% SDS-PAGE. The proteins were transferred to a PVDF membrane and developed with the anti-SCGN antibody (1:10,000).

Recombinant protein purification: Recombinant SCGN was purified from the soluble fraction on a Ni-NTA column followed by gel filtration by modifying the earlier protocol (Sharma et al., 2019b; Khandelwal et al., 2017; Sharma et al., 2015). Briefly, *E. coli* cells

carrying SCGN expressing vector were grown in minimal media. After 10 hours of post induction (0.5 mM IPTG) incubation at 25 ^{o}C, the cell pellet was lysed in Buffer A (50 mM Tris, pH 7.5 and 100 mM KCl). After sonication and centrifugal clearance, the supernatant was loaded onto a Ni-NTA column. Bound protein was washed with 8 column volumes of wash buffer 1 (50 mM Tris, pH 7.5, 100 mM KCl) then with the 10-column volumes of wash buffer 2 (50 mM Tris pH 7.5, 100 mM KCl, 2% Triton X100) followed by a wash with wash buffer 1. Protein was eluted with a gradient flow of elution buffer (50 mM Tris, 100 mM KCl, 50-250 mM imidazole gradient). Pure fractions were subjected to size-exclusion chromatography.

For preparing the Ca^{2+} free protein, the gel filtered protein solution was incubated with a 10x molar concentration of EDTA for half an hour followed by exhaustive buffer exchange with Chelex-purified buffer (50 mM Tris, pH 7.5, 100 mM KCl). For animals and cell culture experiments, the protein was buffer exchanged to PBS, filtered with 0.22 µ syringe filter and aliquots were stored in -80 ^{o}C at 2 mg/ml concentration.

ΔNTD SCGN (amino acid 104-276) and ΔCTD SCGN (amino acid 1-186) were constructed by cloning respective amino acids with appropriate primers into pET21b vector. ΔCTD was purified by anion exchange (Q-Sepharose; Tris, pH 8.5) chromatography while ΔNTD was purified by hydrophobic interaction chromatography (Phenyl-Sepharose; Tris pH 7.5) followed by anion exchange chromatography (Q-Sepharose; Tris, pH 7.5). The details of the truncated protein purification protocol are available on request. All proteins were then subjected to size exclusion chromatography on a Sephadex G-75 (GE Healthcare) column in 50 mM Tris, pH 7.5, 100 mM KCl buffer. Decalcification was essentially same as for the full-length SCGN.

Protein overlay assay: The proteins were immobilized on a PVDF membrane with a slot-blot manifold apparatus (Amersham Biosciences). After blocking with 5% BSA, the membrane was incubated with 10 µM SCGN for one hour and washed four times with PBST. The further procedure was followed as standard Western Blotting with the anti-SCGN antibody (1:10,000 dilution).

To assess insulin binding to truncated SCGN, 10 µM protein samples were immobilized on PVDF membrane. After blocking with 5% BSA, membrane was

incubated with 100 µM insulin. Downstream processing was done as described above except that the anti-insulin antibody was used to probe insulin binding to truncated proteins.

Bio-layer interferometry: BLI experiments were performed on an Octet Red 96 system. Our efforts to immobilize His-tagged-SCGN using Ni-NTA chemistry or using amine-coupling chemistry were unsuccessful because of non-specific binding of insulin to either probe. We hence immobilized insulin (100 µg) on the probe using amine-coupling and 200 µl SCGN (100 µM) was taken as a ligand in the wells in the Ca^{2+} free (100 µM EDTA) or Ca^{2+} saturated (1 mM Ca^{2+}) form. Initial baseline-60 s, association/dissociation- 300 s each followed by a regeneration step. Two controls were run (i) insulin-immobilized probe and buffer in the well, (ii) free inert probe with SCGN in the well. There was an inappreciable signal in the control (i). Reference (ii) was subtracted from the sample. The data fitting was performed for the initial 120 seconds of association phase and 300 seconds of dissociation phase in the vendor-supplied module using 1:1 model. The R^2 of >0.95 and Chi^2 of <1 was used as the criteria of a good fit.

Spectral measurements: Circular dichroism (CD) spectra were recorded on a Jasco J-815 spectropolarimeter using 1 cm path length cuvettes. Fluorescence emission spectra were recorded on an F-7000 Hitachi spectrophotometer at an excitation wavelength of 295 nm. The excitation and emission band passes were set at 5 nm and spectra were recorded in 50 mM Tris (pH 7.5), 100 mM KCl. The spectra were corrected for insulin contribution. Near-UV CD spectra were recorded using 1 mg/ml protein concentration, and fluorescence spectra were recorded using 0.1 mg/ml protein (unless otherwise stated in the graph).

Analytical gel filtration: Differential elution of proteins and their complex were resolved on a Superdex 75 (10/300) column (Wipro GE Healthcare) under described conditions. Column was pre-equilibrated with buffer (50 mM Tris, pH 7.5, 100 mM KCl) containing either 0.1 mM EDTA or 2 mM Ca^{2+}.

Insulin amyloidogenesis by TEM: Either the proteins or their complex were incubated overnight at 60 ºC without stirring. Fibrils thus formed were mixed using a 200 microliter pipette. The solution was applied onto a 300-mesh copper grid and stained with freshly prepared uranyl acetate (2%). Dried samples were observed under a transmission electron microscope (Hitachi, Japan) operating at an accelerating voltage of 200 kV.

Insulin amyloidogenesis and aggregation by fluorescence spectroscopy: For the real-time insulin fibrillation measurement, 85 µM insulin or insulin + SCGN combination (50 mM glycine, 100 mM KCl, pH 2.5, 10 µM ThT) was incubated at 55 ºC (in the absence of Ca^{2+}) or 60 ºC (in the presence of Ca^{2+}) with continuous stirring. ThT fluorescence was monitored for one hour (λ_{ex} =440 nm, λ_{em}=482 nm). For DTT-induced aggregation, 40 µM insulin (in 50 mM Tris buffer, pH 7.5, 100 mM KCl) in the presence or the absence of different concentrations of SCGN was equilibrated at 37 °C for 10 min with constant stirring in the cuvette.. The reduction of insulin was initiated by the addition of 20 mM DTT to the sample. The extent of aggregation was monitored as scattering (excitation and emission monochromators set at 465 nm) set at 5 nm band passes in time scan mode of the instrument.

For a large set of proteins (BSA, full length and truncated SCGN in the presence/absence of SCGN), we measured the extent of insulin fibrillation at regular time intervals while the samples were on a temperature controlled orbital shaker at 300 rpm at 55 ºC (in the presence of 250 µM EDTA) or 60 ºC (in the presence of 1 mM Ca^{2+}). Protein samples were prepared in amyloidogenesis buffer (50 mM glycine pH 2.5, 100 mM KCl, 50 µM ThT) in a 96-well plate. BSA was taken as control (Finn et al., 2012). ThT fluorescence was measured periodically on a Perkin-Elmer multimode Plate reader in triplicate and standard error was calculated from triplicate values.

MTT assay: Fibrils were generated by overnight incubation of 1 mg/ml insulin in 50 mM glycine pH 2.5, 100 mM KCl buffer at 65 ºC. MIN6 cells were seeded at a density of 20,000 cells/well in a 96-well plate. Next day, the cells were washed with PBS and incubated with 10 µM SCGN, 20 µM insulin fibrils (fibrils), a complex of 10 µM SCGN and 20 µM fibrils, 5% Triton X-100 (negative control), or BSA and fibrils complex in serum-free media for 24 hours. Cells were washed again with PBS and incubated with 100

µl of 5 mg/ml MTT in incomplete media for 4 hours at 37 ºC. Fifty microliters of media were replaced with DMSO and mixed properly to dissolve crystals. The absorbance was recorded at 540 nm on a Perkin-Elmer multimode Plate reader. The number of samples per treatment was eight (n=8).

Modelling SCGN-insulin complex- A 3-D model of mouse SCGN was generated by Phyre2 (Protein Homology/analogY Recognition Engine V 2.0) (Kelley et al., 2015) using zebrafish SCGN structure (PDB id: 2Q4U) as a template. mSCGN model was used as a receptor molecule and insulin (PDB 5EN9) was the ligand for generating a docking model by Patchdoc server (Schneidman-Duhovny et al., 2005) while accepting the default settings. The resultant model was analyzed on the Pymol software.

FITC-Insulin preparation: Five-milligram insulin powder was dissolved in 1 ml glycine buffer (50 mM glycine, 100 mM KCl, pH 2.5, 1 mM EDTA) to avoid insulin aggregation. After insulin was dissolved, the solution was diluted 4 times. In parallel, 2 mg FITC was dissolved in 300 µl ethanol. FITC was added drop wise to the insulin solution on a magnetic stirrer in dark at room temperature. After 3 hours of the coupling reaction, the solution was subjected to a size exclusion column attached to a Bio-Rad FPLC system. Pure insulin fractions were decided by the absorbance at 280 and 495 nm set in a Quadtec detector. The extent of FITC conjugation was calculated exactly as recommended by the SIGMA (CAS #: 3326-32-7). Our preparation was found to have ~4 FITC molecules per insulin molecule.

FACS assisted quantification of 2-NBDG: HepG2 cells were cultured in six-well plates. After cells reach ~80% confluency, cells were kept in glucose-free KRP buffer for overnight fasting/glucose deprivation. Subsequently, cells were subjected to the following treatment: 40 µM 2-NBDG, 100 nM insulin, 100 nM SCGN, a complex of SCGN and insulin in glucose-free KRP buffer for 2 hours. Control samples did not receive any treatment except the corresponding buffer. The cells were washed with PBS and processed for FACS analysis essentially as described in the previous section.

Microscopic and FACS study of FITC-insulin internalization: HepG2 cells were seeded on the coverslips in a six-well plate **(**$0.2x10^6$ cells/well). After cells reached ~80-90% confluency, the cells were serum deprived for 24 hours and were treated with 10 µM FITC-insulin either in the presence or absence of 10 µM of unlabelled SCGN. After 30 min incubation, the culture plate was transferred to the ice and was washed thrice with ice-cold PBS followed by two washes with ice-cold glycine-NaCl buffer (120 mM glycine, 150 mM NaCl, pH 2.5) to remove membrane-bound FITC-insulin. After additional two washes with ice-cold PBS, cells on coverslips were fixed and mounted on a glass slide with DAPI containing mounting media. For better visualization, DAPI was pseudo-colored to red instead of conventional blue color. The images were captured on an Apotome 2 system with 63x objective and oil immersion medium. The exposure time for each channel was constant for all the samples. No image processing was performed on the acquired images.

For FACS-assisted quantification of FITC-insulin internalization, samples were prepared similarly except that coverslips were not used for FACS samples. After the washes, the cells were trypsinized, centrifuged and the cell pellet was resuspended in 400 µl PBS. Immediately, FACS analysis was performed on a Beckman Coulter Gallios Flow Cytometer system using FITC channel. At least 20,000 cells were analyzed for each sample. The data analysis and figure preparation were performed by Kaluza software module provided by the vendor.

ELISA for insulin internalization: HepG2 or N2A cells (0.2 million cells/well) were seeded in a six well plate. After 24 hours, serum free mediated containing 100 ng/ml insulin alone or with 1 µg/ml SCGN was added to three wells. After one hour of incubation, mediated samples were taken and were used for ELISA quantification of free insulin in media.

Akt phosphorylation assay: C2C12 cells were differentiated in T25 cell culture flasks. Differentiation was induced by incubating C2C12 myoblast in serum free media supplemented with 100 nM insulin. After 24 hours, the cells were incubated in serum free media for another 48 hours which leads to differentiated C2C12 myotube formation (Fig. S12). After glucose deprivation (2 hours for C2C12 and 4 hours for HepG2 cells) in

glucose-free KRP (20 mM HEPES, 0.4 mM K_2HPO_4, 1 mM $MgSO_4$, 5 mM KCl, 135 mM NaCl), the cells were washed thrice and treated with insulin (100 nM) or SCGN (100 nM) or with a complex of the two in KRP buffer. Control samples received the corresponding buffer. After 20 minutes, cells were lysed in RIPA buffer. Total protein was quantified by BCA method and 50 µg protein was resolved on two parallel 12% SDS-PAGE gels followed by Western blotting. One blot was processed for pAkt (Ser473) antibody (1:10,000) while other blot was used for co-detection of β-actin (1:10,000) and Akt (1:10,000) with respective antibodies. Densitometry analysis was performed with Image J software. The pAkt/Akt values were first normalized with corresponding actin values and then a ratio of normalized pAkt/Akt was calculated using Microsoft excel software.

Animal maintenance, OGTT and ITT: Animals (after due approval from the Institutional Animal Ethics Committee, approval numbers 91/2015, 2/2017 and 35/2017) were maintained in *Individually Ventilated Cages. BALB/c* mice were kept *on normal chow, C57BL/6J mice were fed either normal chow (control group) or HFD. To induce diabetes in BALB/c* mice, STZ (100 mg/kg bodyweight in citrate buffer pH 4.5) was injected intraperitoneally after six hours of fasting. After 3 days, glucose level was measured and animals showing random glucose >200 mg/dL were selected for experiments. *C57BL/6J* mice were maintained on a high-fat diet (HFD; D12492, Research Diets, New Brunswick, NJ) or normal chow and the SCGN treatment was started simultaneously. After three months, the first set of OGTT and ITT experiments were performed.

OGTT was conducted after overnight fasting. Mice were fed an oral bolus of 2 g glucose per kilogram body weight and blood glucose was monitored at every 30 min using an AccuCheck active OneTouch glucometer (Roche).

ITT was conducted after 6 h of fasting. Mice were injected with (i.p.) 0.75 IU of fast acting insulin per kilogram body weight and blood glucose was monitored at every 20 min using an AccuCheck active OneTouch glucometer (Roche).

Serum Analysis: Random triglyceride (GPO/PAP method, TG kit, Coral Clinical Systems), cholesterol (CHOD/PAP method, CHOL Kit, Coral Clinical Systems), HDL (Direct enzymatic method, HDL-D kit, Coral Clinical Systems), Ca^{2+} (OCPC method,

CAL Kit, Coral Clinical Systems) and glucose (Glucose (GO) assay kit; cat: GAGO20-1KT, SIGMA) were measured as per the product guidelines and protocols. LDL level was calculated by the equation: (Total Cholesterol) – (HDL) – (TG/5).

ELISA: Insulin (Ultra-Sensitive Mouse Insulin ELISA kit, Crystal Chem; cat: 90080) and SCGN (Secretagogin BioAssay™, USBiological; cat: 027968) measurements were performed as per the vendor's guidelines following the product protocols.

Insulin sensitivity index [$ISI_{(0,\ 120)}$]: The insulin sensitivity index was calculated precisely as described (28). Briefly, after 16 hours of fasting, blood was drawn for serum insulin/glucose measurements. Two hours after the oral glucose bolus (as described in OGTT), another sample of blood was collected. Serum glucose and insulin levels were determined as described in respective sections. Metabolic Clearance Rate (MCR) and Mean Serum Insulin (MSI) were calculated and insulin sensitivity was calculated as $ISI_{0,120}$= MCR/log MSI.

Oil Red O staining: Frozen liver tissues were sectioned on a microtome at the thickness of 5 micrometers and immobilized on charged slides. Oil Red O (SIGMA, O1391-250ML) staining was performed as follows. Tissues were soaked in distilled water followed by a wash with PBS. Then slides were dipped in 60% isopropanol followed by immersion in Oil Red O solution for 1 hour. Next, slides were washed twice with PBS (5 min each) followed by immersion in hematoxylin solution for 4 minutes. Finally, slides were washed in running tap water and glycerol soaked tissues were covered with coverslips. Slides were observed under an Axioplan 2 imaging system. Quantitation of oil red stained pixels was performed using ImageJ software. Three animals were arbitrarily selected from each group. For every sample, ORO^{+} pixels from seven fields were average. Students t-test was performed on averaged values (*i.e.* n=3).

Echo-MRI: EchoMRI™-500, which is designed to analyze the body composition for live small animals, was used for total fat content measurements. Animals were maintained in vendor provided animals restrainer. All readings were the average of three accumulations.

Histology: At the end of experiments (and after a recovery period), animals were sacrificed using recommended procedures. Tissues were excised and fixed in formalin (10% formaldehyde in phosphate-buffered) followed by processing and embedding. The paraffin-embedded tissues were sectioned at 4-micrometer thickness. Sections were stained with hematoxylin and eosin and were visualized on an Axioplan 2 imaging system.

qRT-PCR: Tissue samples, immediately after removal from animals, were washed and immersed in TRIzol RNAiso plus reagent and stored at -80 ºC. At the time of processing, tissues were thawed and total RNA was isolated by chloroform extraction. Upon checking the integrity and concentration of RNA, 5 µg of RNA was used for cDNA synthesis using SuperScript III First-Strand Synthesis System (Thermo Fisher Scientific). mRNA levels were quantified by qRT-PCR (ABI Prism 7900 HT; Applied Biosystems) using SYBR Green (Applied Biosystems). The primer sequence for analyzed genes is appended in the supplementary information (Table. S1).

Statistical analysis: All significance tests for group-wise comparison were performed on MS excel using student's t-test except OGTT and ITT time course measurements where two-way ANOVA analyses (with Holm-Sidak post-hoc analysis) were performed on the Sigma plot software.

Supplementary references

Kelley LA, Mezulis S, Yates CM, Wass MN, Sternberg MJE (2015) The Phyre2 web portal for protein modeling, prediction and analysis. *Nature Protocols,* 10, 845-858.